



DEM Modeling of the Influence of vibrational forcing on the flowability of milled biomass in wedge-shaped hoppers



Nick Deak¹, Hariswaran Sitaraman¹, Yimin Lu², Nepu Saha³, Jordan Klinger³, Yidong Xia³

¹National Renewable Energy Laboratory

²Texas Tech University

³Idaho National Laboratory

Aug. 13, 2024

Feedstock variability

- Variable milled biomass feedstocks can pose operational challenges in biorefineries
 - Arching, ratholing, surging flow in hoppers
 - Clogging/jamming in screw conveyors
- Such disruptions impact refinery production and profitability
- From Williams (2016), feedstock flowability impacted by:
 - Particle morphology
 - Moisture content/cohesiveness
 - Compressibility
 - Bulk density



Milled corn stover



Switchgrass, Guo (2020)



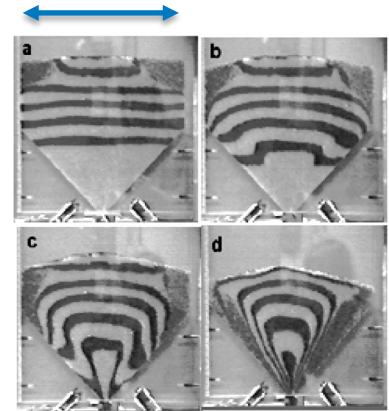
Pine chips, Xia (2019)

Vibrational forcing

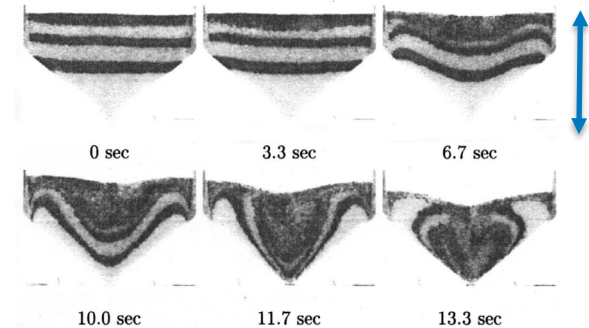
Vibrational forcing used as a strategy for inducing and maintaining particle flow in hoppers

- Hunt, Wassgren et al. found that horizontal and vibrational forcing strategies could induce different flow patterns (right)
- Janda et al. observed that the arching distance could be decreased to approximately one particle diameter with sufficient forcing
- Such studies have been limited to simple, often uniform particle types, little to no data exists for complex milled biomass

Objective: Use DEM to investigate how horizontal and vertical vibrations applied to a hopper impact the flowability of milled biomass



Flow patterns under the influence of horizontal vibrational forcing (Hunt et al., 1999)



Flow patterns under the influence of vertical vibrational forcing (Wassgren et al., 2002)

BDEM implementation

An open-source GPU-accelerated DEM solver



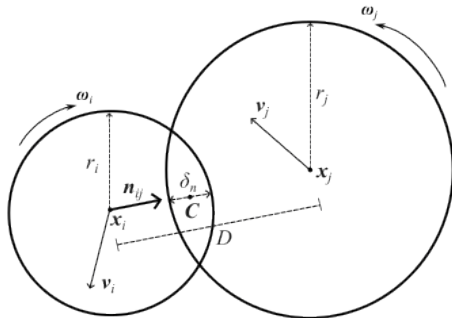
<https://github.com/NREL/BDEM>

BDEM – a biomass DEM solver

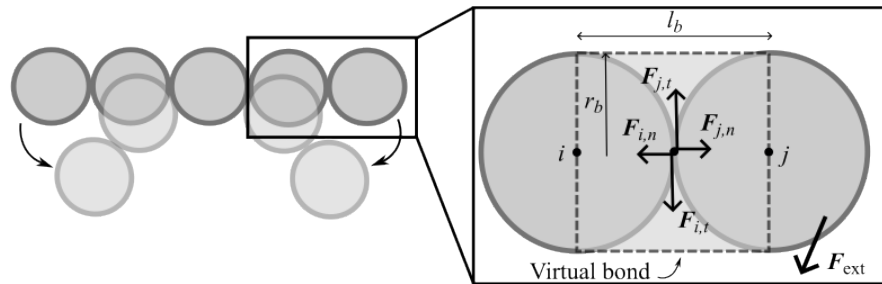
BDEM is an open-source massively-parallel DEM solver that specializes in biomass handling problems

- Supports linear spring-dashpot (LSD) and Hertz-Mindlin (HM) contact models
- Includes glued and bonded-sphere models for complex particle shapes
- Particle cohesion captured using liquid bridge and SJKR models

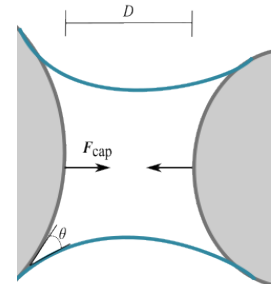
LSD and HM contact models



Bonded sphere model

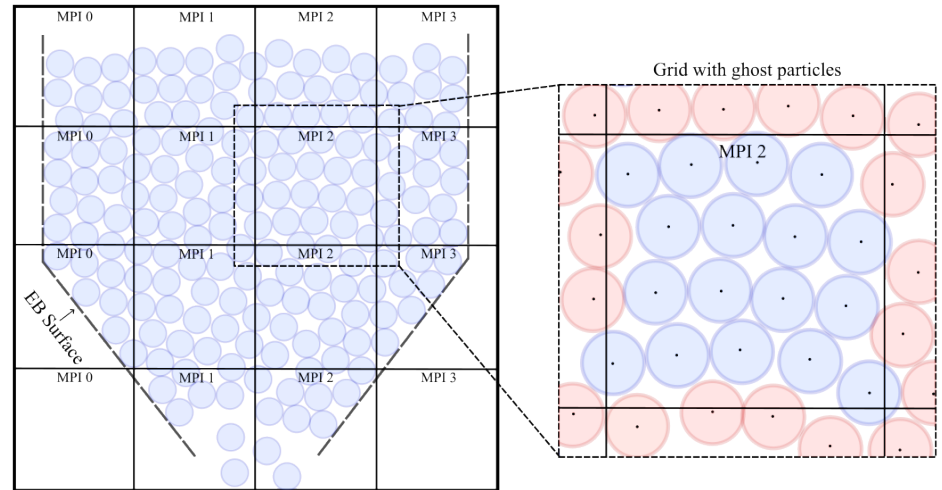


Liquid bridge model



Parallel implementation

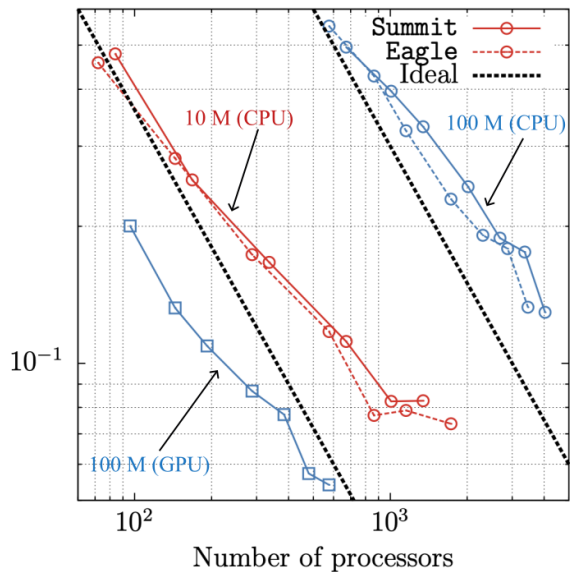
- **BDEM** is built on top of the AMR library AMReX, and supports hybrid CPU/GPU parallelization
- The domain is discretized into grids, which are assigned to individual MPI ranks/GPUs
- Each grid includes ghost particles to ensure collisions between particles in neighboring grids are included
- BDEM also support complex moving geometries



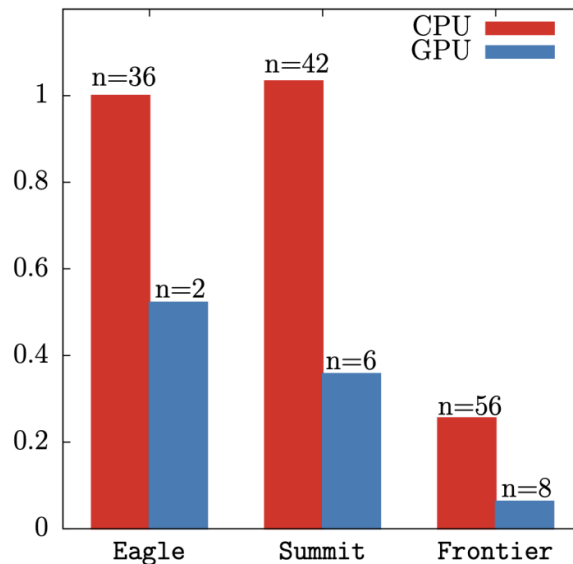
Parallel performance

- Excellent scaling performance on multiple HPC systems on problem sizes $> O(100 \text{ M particles})$
- GPU speedup of 2-4x observed on systems tested

Wall-clock time/step (s)



Execution time



BDEM validation

Hopper discharge experiments



- Hopper discharge experiments with 4 mm corn stover performed at INL with MC 10-30%
- Hopper opening varied to find arching distance



Challenge

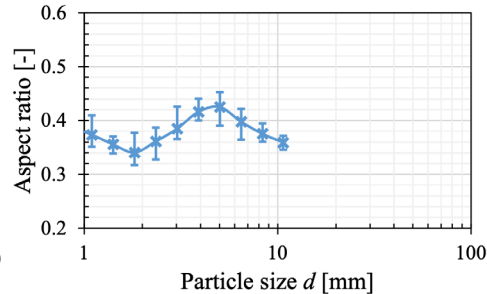
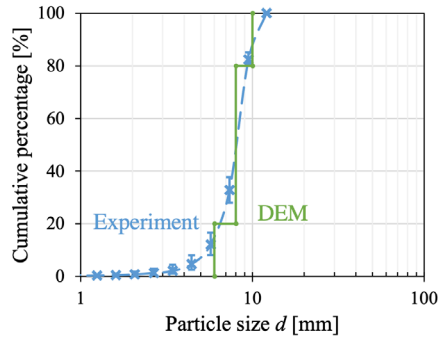
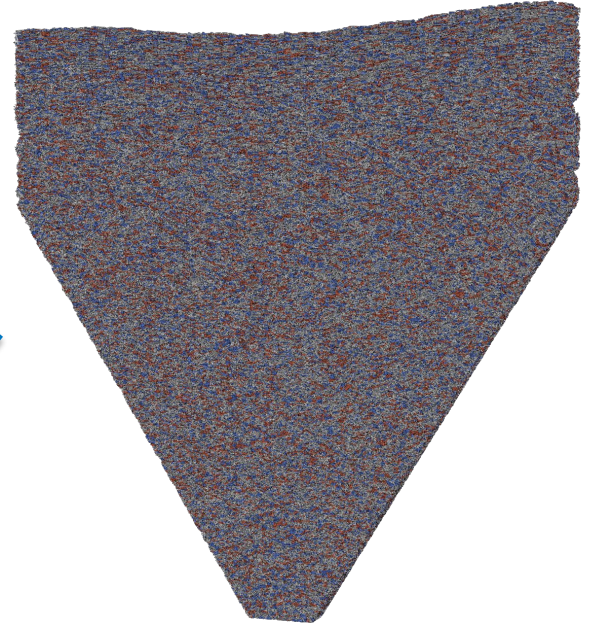
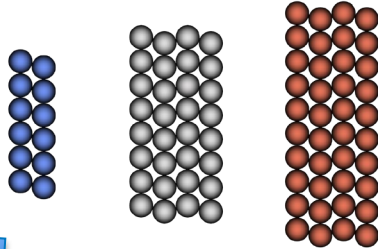
No-flow behavior observed up until very large openings ($W \sim 90$ mm) - need to recreate behavior with BDEM

Particle conceptualization

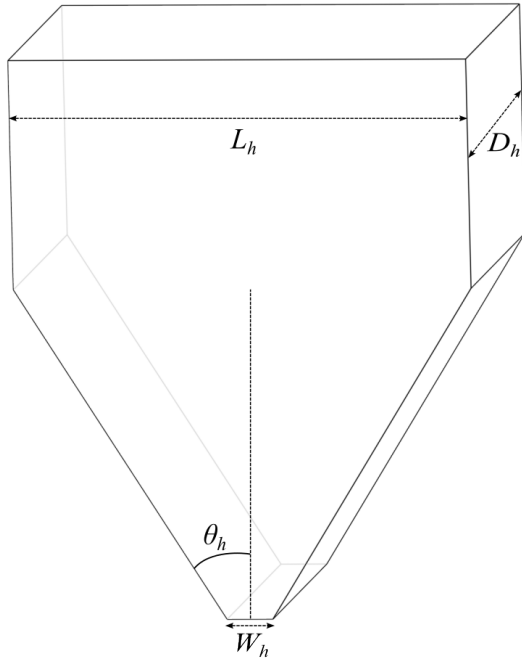
4mm whole corn stover



Corn stover particle types

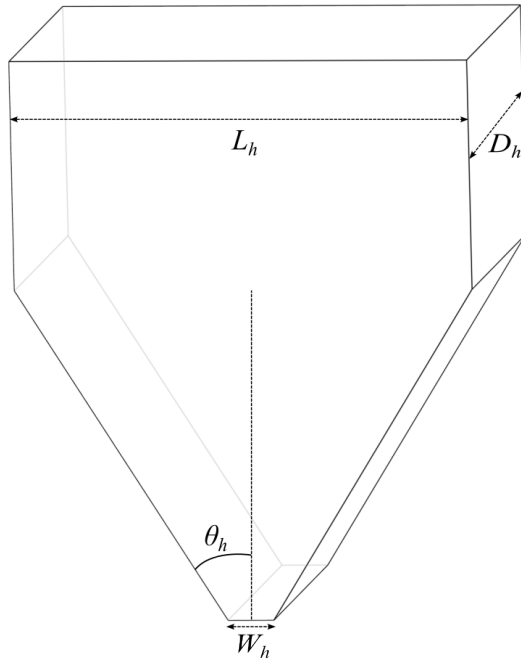


Simulation setup



Parameter	Value
<i>Hopper parameters</i>	
Hopper bin width (L_h)	0.6 (m)
Hopper bin depth (D_h)	0.03125 (m)
Hopper exit size (W_h)	90 (mm)
Fill height (H)	0.45 (m)
Inclination angle (θ_h)	32°
Wall Young's modulus (E_w)	10 ⁹ (Pa)
<i>Particle parameters</i>	
Particle Young's modulus (E_p)	5 × 10 ⁵ (Pa)
Particle Poisson's ratio (ν_p)	0.3
Particle radius (r)	0.5 (mm)
Particle density (ρ)	215 (kg/m ³)
Normal restitution coefficient (e_n)	0.1
Particle-particle friction coefficient (μ_p)	0.9
Particle-wall friction coefficient (μ_w)	0.9
<i>Bond parameters</i>	
Bond normal stiffness (k_n^b)	10 ⁸ (N/m ³)
Bond tangential stiffness (k_t^b)	6 × 10 ⁶ (N/m ³)
Bond radius (r_b)	0.5 (mm)
<i>Cohesive model parameters</i>	
Liquid bridge contact angle (θ)	0°
Liquid bridge surface tension (γ)	0.073 (N/m)
Moisture content (MC)	10%
Fiber saturation point (FSP)	0%
Liquid bridge viscosity (η_v)	10 ⁻³ (Pa-s)
Cohesive energy density (CED)	10 ⁴ (J/m ³)

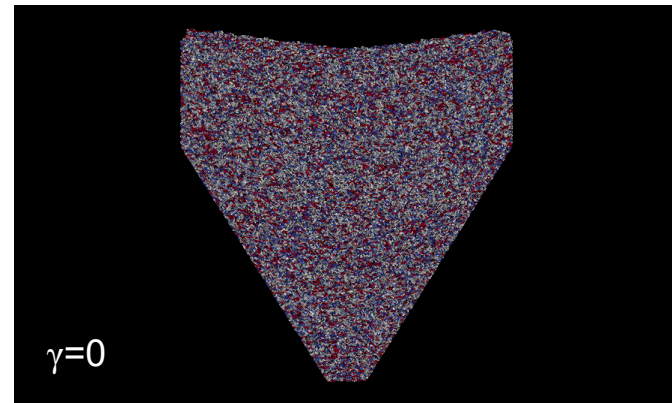
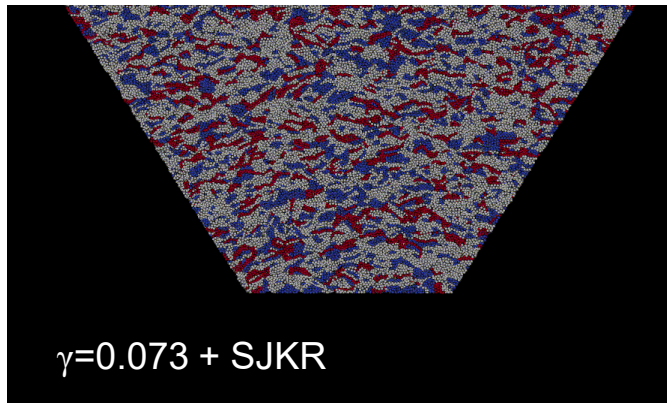
Simulation setup



Parameter	Value
<i>Hopper parameters</i>	
Hopper bin width (L_h)	0.6 (m)
Hopper bin depth (D_h)	0.03125 (m)
Hopper exit size (W_h)	90 (mm)
Fill height (H)	0.45 (m)
Inclination angle (θ_h)	32°
Wall Young's modulus (E_w)	10 ⁹ (Pa)
<i>Particle parameters</i>	
Particle Young's modulus (E_p)	5 × 10 ⁵ (Pa)
Particle Poisson's ratio (ν_p)	0.3
Particle radius (r)	0.5 (mm)
Particle density (ρ)	215 (kg/m ³)
Normal restitution coefficient (e_n)	0.1
Particle-particle friction coefficient (μ_p)	0.9
Particle-wall friction coefficient (μ_w)	0.9
<i>Bond parameters</i>	
Bond normal stiffness (k_n^b)	10 ⁸ (N/m ³)
Bond tangential stiffness (k_t^b)	6 × 10 ⁶ (N/m ³)
Bond radius (r_b)	0.5 (mm)
<i>Cohesive model parameters</i>	
Liquid bridge contact angle (θ)	0°
Liquid bridge surface tension (γ)	0.073 (N/m)
Moisture content (MC)	10%
Fiber saturation point (FSP)	0%
Liquid bridge viscosity (η_v)	10 ⁻³ (Pa-s)
Cohesive energy density (CED)	10 ⁴ (J/m ³)

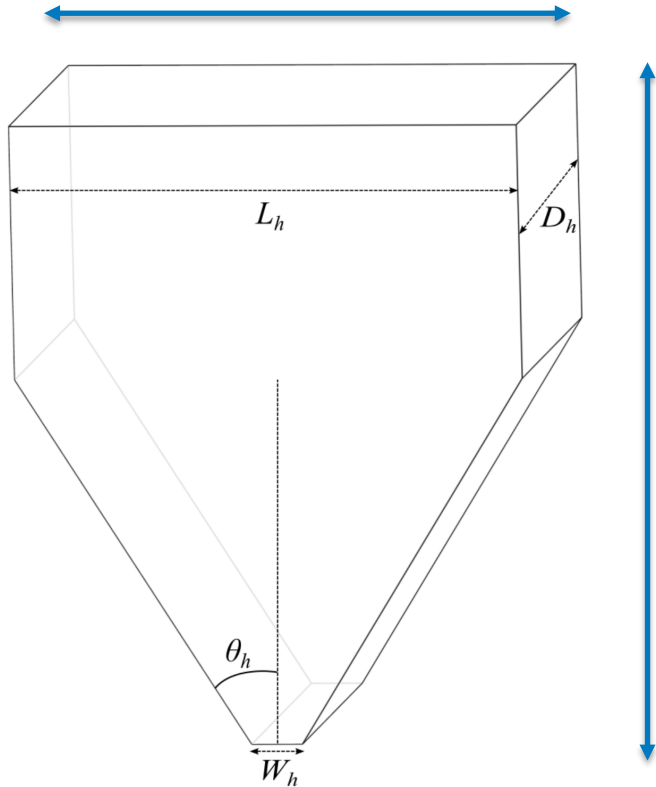
Hopper discharge results

- Smooth discharge observed when liquid bridges were neglected (even with artificially high friction coef.)
- Results indicate that expected no-flow behavior only achieved when both liquid bridges and SJKR cohesion models are used simultaneously



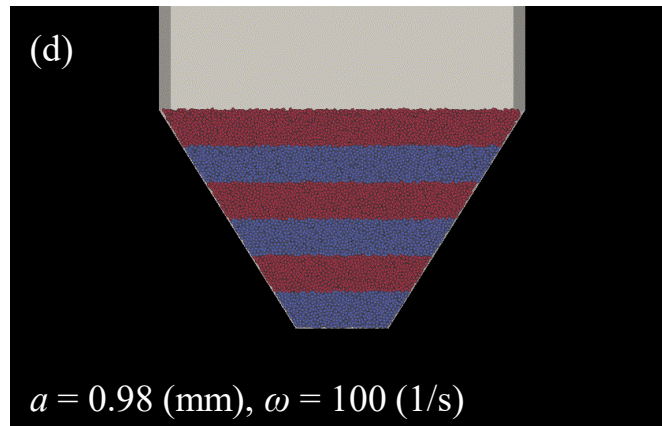
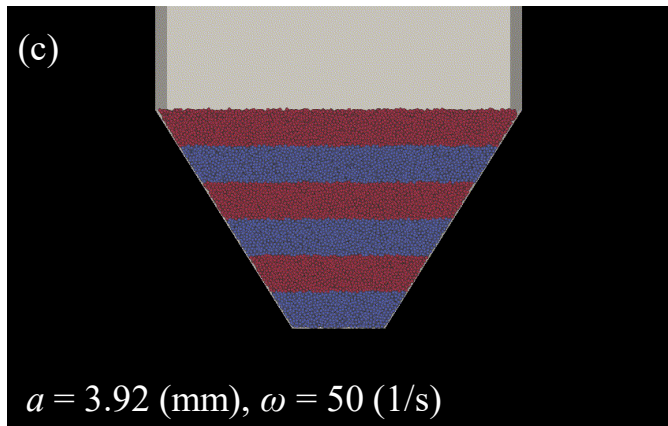
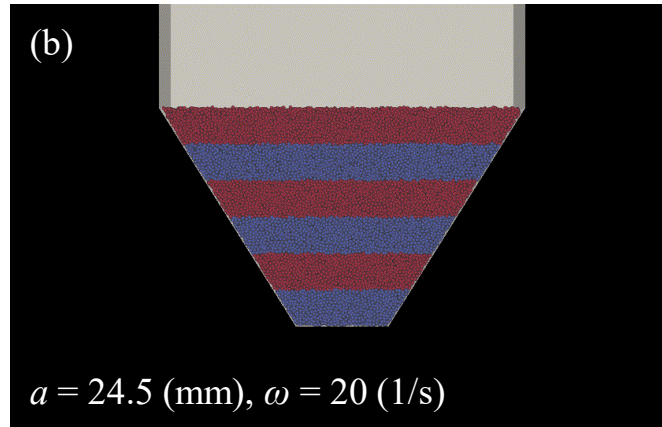
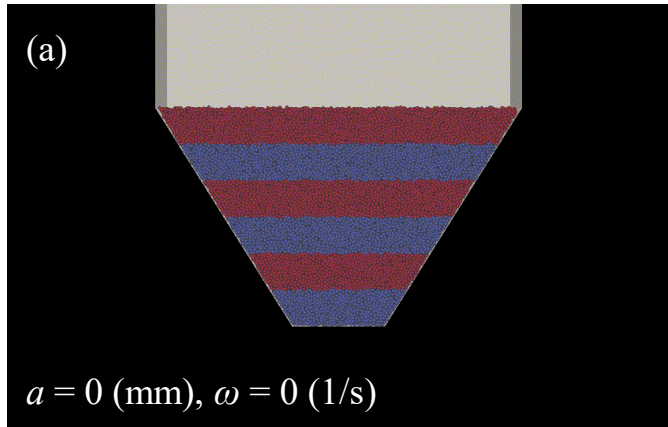
Vibrational forcing simulations

Problem Configuration



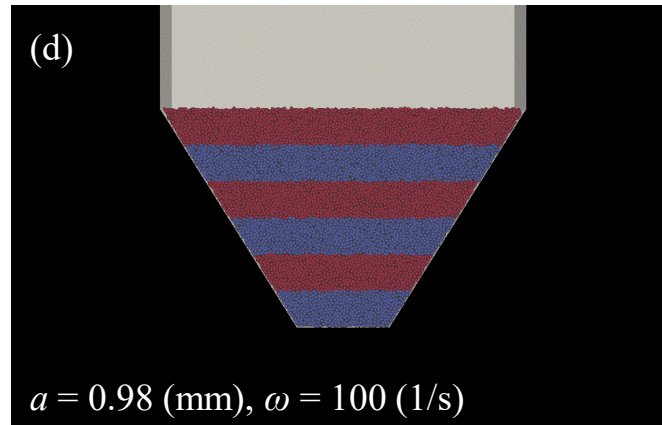
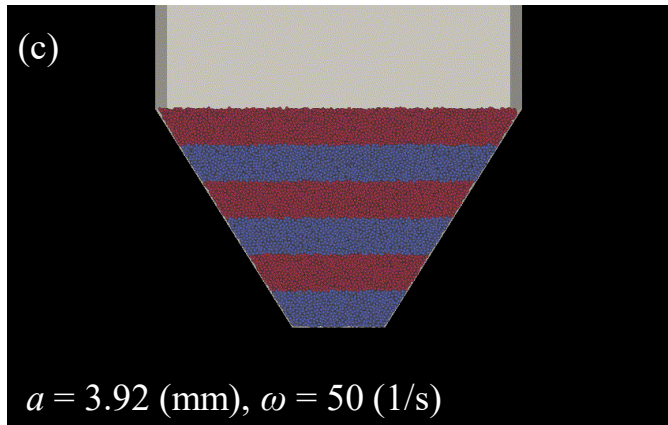
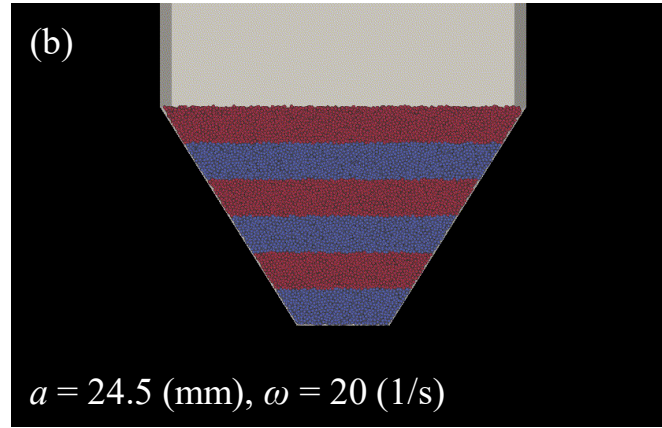
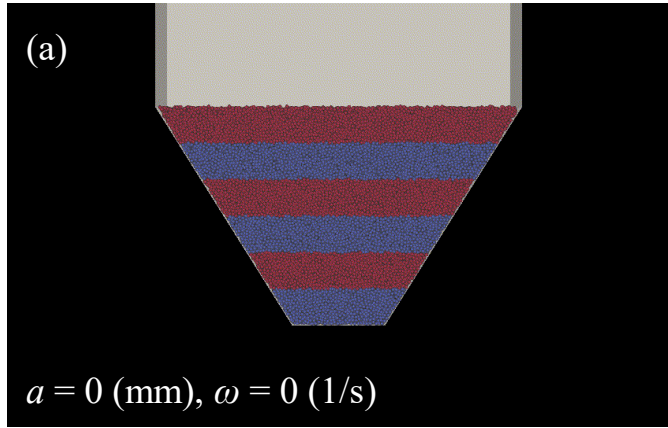
- Wedge hoppers (initially closed) are filled with corn stover particles and brought to rest, small and large configurations explored
- Hopper exit is opened, and sinusoidal vibrations are applied to hopper
 - Horizontal and vertical vibrations are explored
- Dimensionless vibrational acceleration defined as $\Gamma = a\omega^2/g$
 - a is the vibration amplitude
 - ω is the vibration frequency
- Parameter ranges: $1 \leq \Gamma \leq 4$
 - $15 \leq \omega \leq 400 \text{ s}^{-1}$
 - $0.1 \leq a \leq 50 \text{ mm}$

Horizontal vibrations ($\Gamma = 1$)



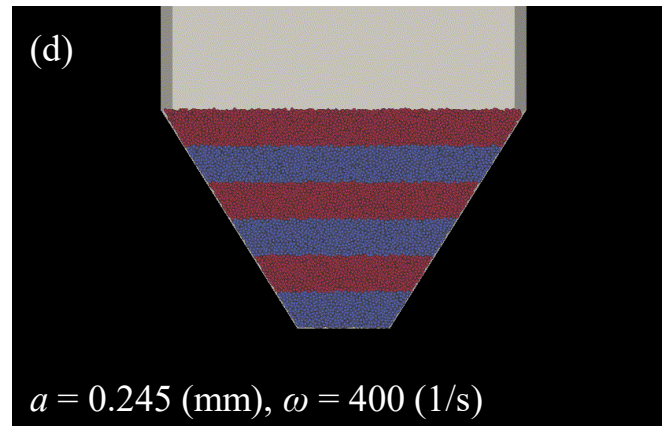
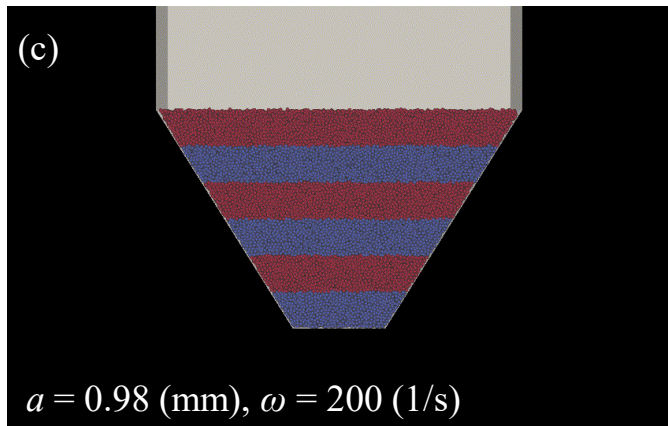
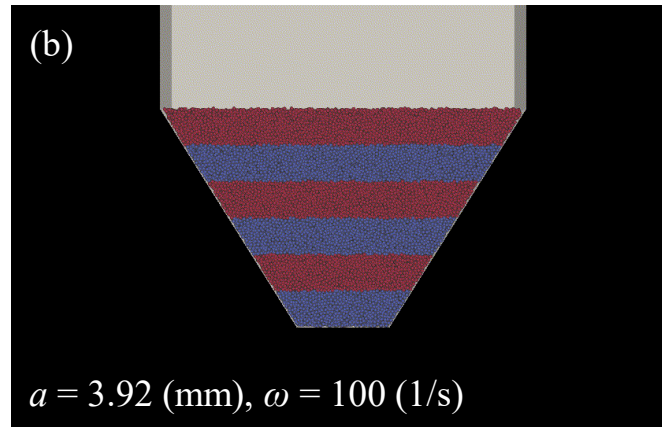
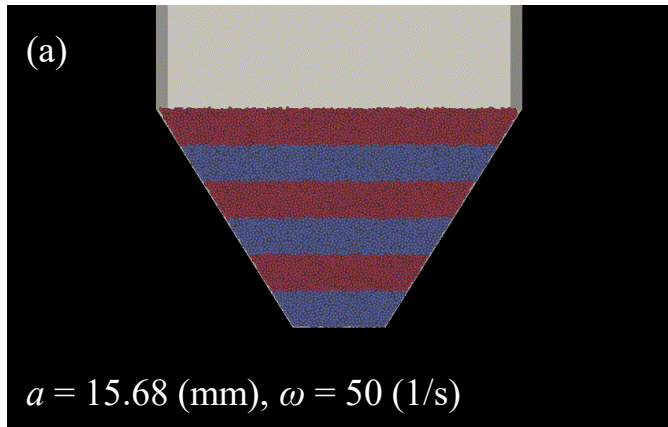
- Discharge times:
 - (a): 17.50 s
 - (b): 2.10 s
 - (c): 6.10 s
 - (d): 9.60 s

Vertical vibrations ($\Gamma = 1$)



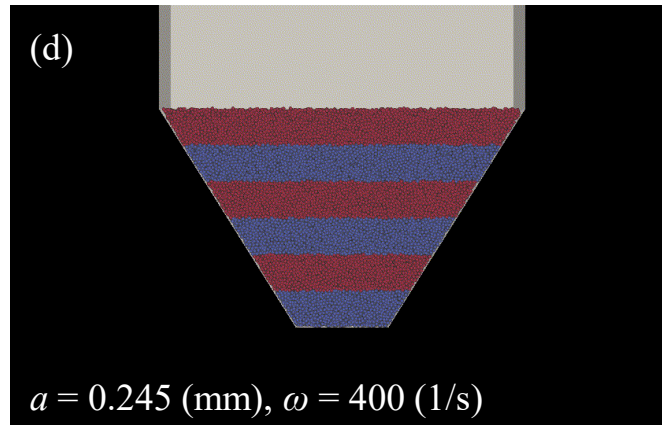
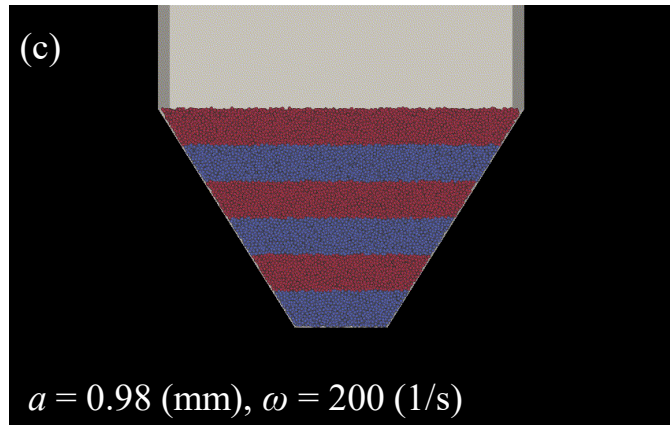
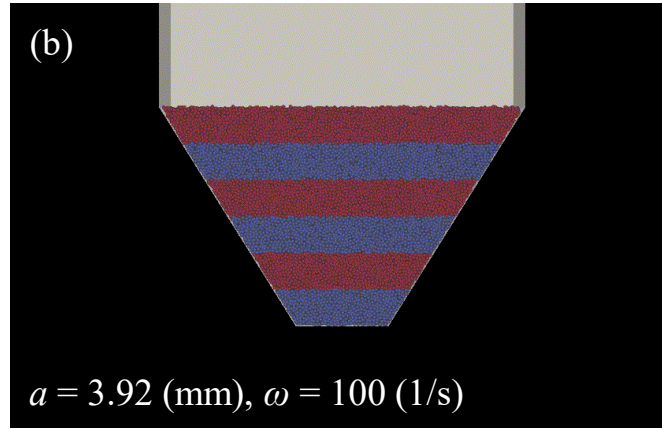
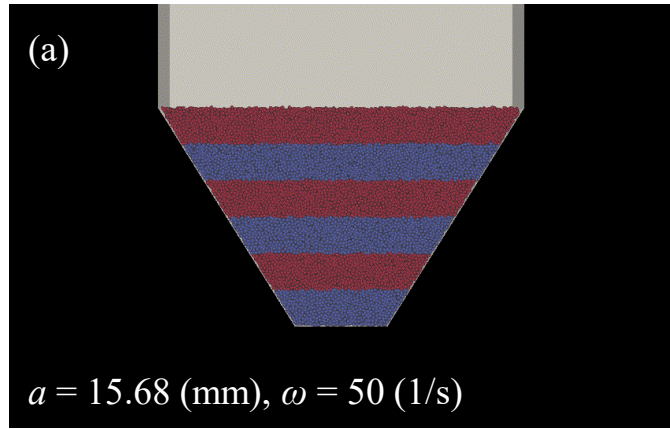
- Discharge times:
 - (a): 17.50 s
 - (b): 1.65 s
 - (c): 4.65 s
 - (d): 9.35 s

Horizontal vibrations ($\Gamma = 4$)



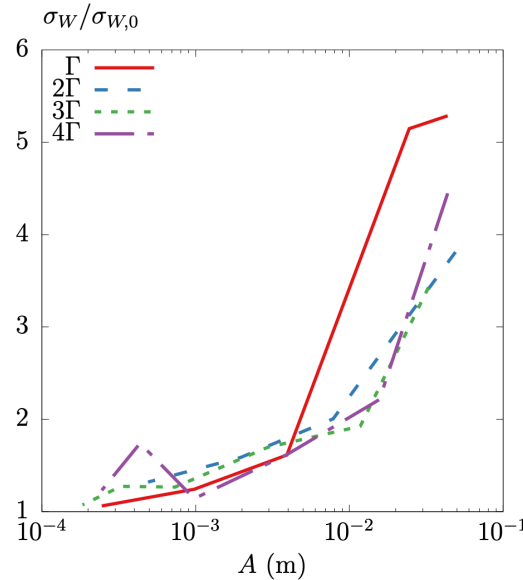
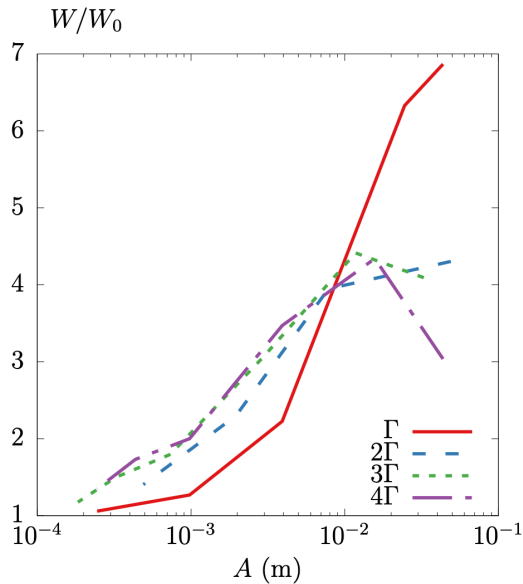
- Discharge times:
 - (a): 3.70 s
 - (b): 3.95 s
 - (c): 6.90 s
 - (d): 7.85 s

Vertical vibrations ($\Gamma = 4$)



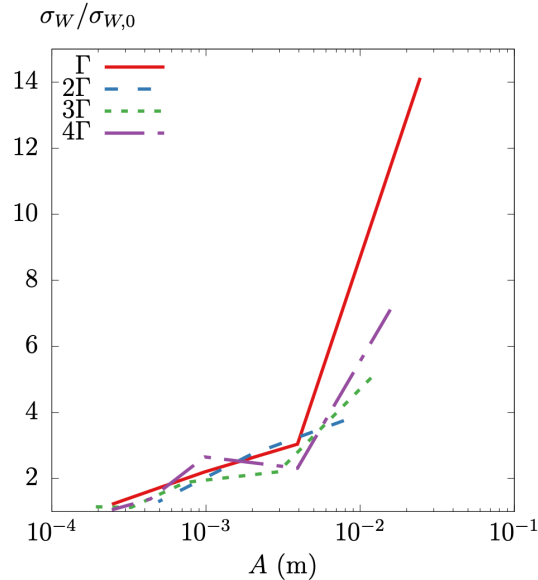
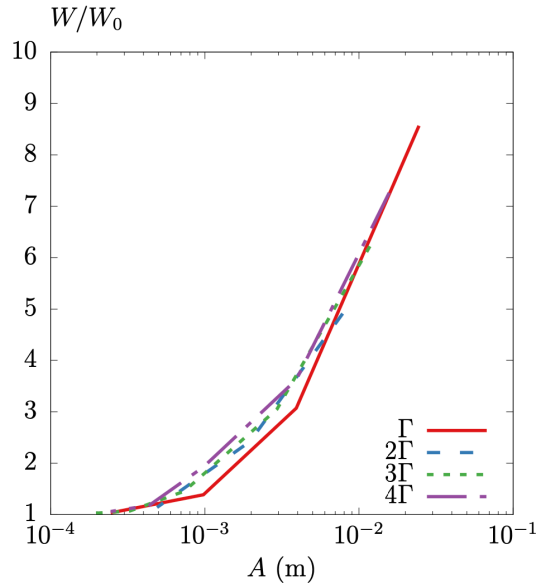
- Discharge times:
 - (a): 1.80 s
 - (b): 3.80 s
 - (c): 8.75 s
 - (d): 10.25 s

Horizontal vibration results



- Any vibrational forcing yields increased flow rate over base case
- Flow rate primarily function of amplitude a
 - Frequency ω has a secondary effect
- Local maximum in discharge rate observed around larger a values
- Larger vibrations lead to greater intermittency

Vertical vibration results



- Discharge rate becomes a function of a only
- Compared against horizontal vibrations, discharge rates larger for a given a and ω
- Greater intermittency also observed (vs. horizontal) for large amplitudes
- The observed trends were present for both the small and large hoppers

Conclusions

- Development of an open-source high-performance DEM solver capable of representing complex particles
- BDEM successfully replicated no-flow behavior with complex particle shapes and liquid bridge cohesion
- Simulations demonstrated that discharge rate and flow intermittency largely governed by forcing amplitude
- For a given forcing amplitude and frequency, vertical vibrations generally induce higher flow rates
- Flow fields did not differ considerably across cases
- Hopper size had little impact suggesting results may hold for scaled-up cases

Collaborators

NREL:

- Hariswaran Sitaraman

INL:

- Yidong Xia
- Wencheng Jin
- Jordan Klingner
- Nepu Saha
- Tiasha Chattarjee

ANL:

- Oyelayo Ajayi

LANL:

- Benjamin Davis
- Ricardo Navar

Texas Tech:

- Yimin Lu



Thank You!

www.nrel.gov

This work was authored in part by the National Renewable Energy Laboratory, operated by Alliance for Sustainable Energy, LLC, for the U.S. Department of Energy (DOE) under Contract No. DE-AC36-08GO28308. Funding provided by U.S. Department of Energy Office of Energy Efficiency and Renewable Energy Bioenergy Technologies Office. The views expressed in the article do not necessarily represent the views of the DOE or the U.S. Government. The U.S. Government retains and the publisher, by accepting the article for publication, acknowledges that the U.S. Government retains a nonexclusive, paid-up, irrevocable, worldwide license to publish or reproduce the published form of this work, or allow others to do so, for U.S. Government purposes.

